25th ABCM International Congress of Mechanical Engineering
October 20-25, 2019, Uberlândia, MG, Brazil

COBEM-2019-1255
AUTOMATIC INSPECTION OF CYLINDRICAL FASTENERS USING 2D LASER SCANNER FOR ROBOTIC CELL

Kleber Roberto da Silva Santos
UNIFEI – Universidade Federal de Itajubá – 1303 BPS Ave, Itajubá,/MG, 37500-909, Brazil
santoskr@unifei.edu.br

Gustavo de Melo Carvalho
Rodrigo Tanure Tricarico
Luiz Fernando L. Rocha Ferreira
Emília Villani
ITA – Instituto Tecnológico de Aeronáutica – 50 Marechal Eduardo Gomes Square, São José dos Campos/SP, 12228-900, Brazil
gumelo@ita.br; rodrigotanure@ccm-ita.org.br; luiz.ferreira@ccm-ita.org.br; evillani@ita.br

Abstract. *The paper presents the comparative test between computational algorithms, linear scanning trajectories and target positioning to identify the distance between centers of cylindrical fasteners installed in a flat test board through the analysis of a three-dimensional point cloud matrix. The scanning point cloud is generated experimentally in an automated way using a 2D laser scanner sensor attached to a 7DOF industrial robotic manipulator. The manipulator performs linear movements in the Y direction, with determined steps and no overlapping of scanned regions in two different way, while the sensor captures the distances in the X and Z direction between its sensor region and the surface in front of it. Four computational algorithms were tests to extraction of center position and distance between centers. To evaluate the methodology created, a three-factor factorial experiment was designed to prove the effectiveness of the method and select the best configuration of techniques to minimize the measurement error. The results show that the methodology was able to estimate the distance between centers and the best set of identified factors presented a median error around 0.04mm and variability of 0.18mm, proving the effectiveness of the method.*

Keywords: *Automated inspection, point cloud, industrial robotic manipulators, 2D laser scanner, 3D scanning, design of experiments (DoE).*

1. INTRODUCTION

Surface scanning has proved to be viable as an industrial inspection technique because it allows the measurement of dimensional parameters without the need for contact with the part and because it is more easily automated. With the miniaturization of the scanners sensors and the increase of the processing capacity of the industrial controllers, it is already possible to incorporate these sensors into the effectors of manipulators in operation in the industry, adding in its operation the dimensional measurement function without prohibitively affecting yours working time cycle.

In the literature, it is possible to identify some works within the theme of scanning inspection. In Lavrinov and Khorkinn (2017) and Di Angelo et al. (2019) point cloud generated by 3D scanning are used to identify dimensional parameters of products. Lavrinov and Khorkinn (2016) discusses the calibration of 2D scanner sensors by triangulation. In Chu et al. (2018) a 2D scanner similar to the one used in this work is used, but the handling platform has 2DOF (*Degree of Freedom*) with linear axes, being the article focus the 3D object reconstruction. A 6DOF industrial robotic manipulator with a 2D scanner is used in Phan et al. (2018), and the focus of this article is the generation of the robot manipulator trajectory in order to cap the entire topology of the surface, there is a concern with scan overlay control to generate a consistent model. A 6DOF industrial robotic manipulator is also adopted in Rao et al (2018) but is using a structured light scanner for dimensional measuring. In Zhang et al. (2017) 2D scanner is embedded in a quadruped robot for identifying human beings, with the point cloud formed by the reading scanner and pan-tilt variation provided by the robot.

Several applications are studied in this area, as in medicine (Haleem and Javaid, 2018); high-voltage tower inspection by drones (Viña and Morin, 2017), mobile-based robotics (Cao et al., 2009) and (Huhle et al., 2011); autonomous cars (Wang and Liu, 2016); inspection of road defects (Yamada et al., 2014), among others.

This work aims to validate the use of 3D scanning with a poor cloud of points to identify the distance between centers of cylindrical fastener installed in a flat plate. It uses a point cloud generated experimentally in an automated way by the integrated operation of a 2D scanner and an industrial robotic manipulator. In the two adopted scanning

strategy, there are no overlap of scanning regions which causes a loss of information from the point cloud compared to real surface. Four computational methods are used to identify the desired dimensional parameters, and they are compared with a measurement of the test board made in a CMM (Coordinate-Measuring Machine). It is also investigated whether the scanning position of the target to be identified has influence on the dimensional parameter to be found.

2. METHODOLOGY

The test bench is the same as described in (Santos et al., 2018) which briefly consists of a 7DOF industrial robotic manipulator model Kuka LBR IIWA 14 820, a distance measuring sensor model OCP662P0150E from the manufacturer Wenglor, a 2D laser scanner sensor Model LLT26-100 from Micro Epsilon Manufacturer. Such sensors are attached of the robotic manipulator handle through a specially designed effector, as show in Fig. 1a, 1b and 1c.

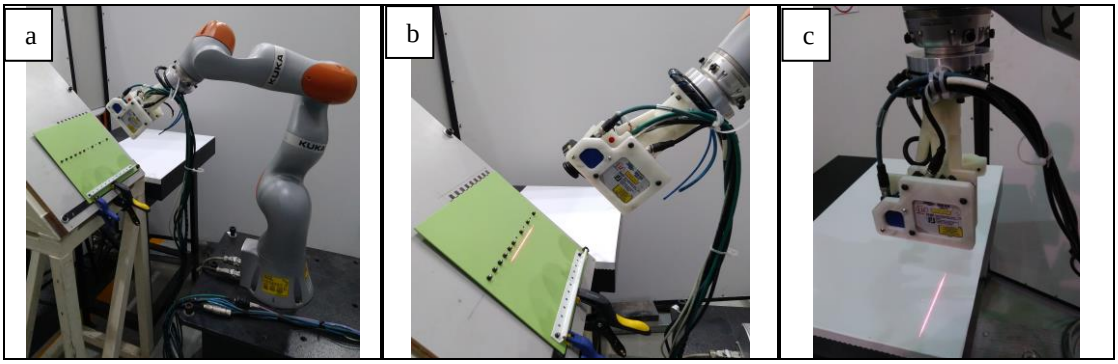

Figure 1. (a) Experimental Assembly; (b) and (c) 2D laser scanner fixed into robotic manipulator (Santos et al.,2018).

All devices communicate to a desktop computer with Intel® core i7-7740X processor with 32Gb RAM through the TCP/IP protocol. A software developed in Labview® is responsible for coordinating the operation of all the equipment to perform the routine of surface scanning, generating a three-dimensional cloud point matrix that is analysed by the software to extract the desired dimensional information. In Figure 2d and 2e can be seen the visualization of the point cloud matrix generated from test board scan after data processing. The test board was a flat plate with twenty-seven fasteners fix in it, arranged in nine rows and three columns, as is show in Fig. 2a. The scanning was done by line, as show in Fig. 2b. In Figure 2c is show scan reference system and the identification number of the fasteners in the specimen. The position of the scanning reference system was chosen non-symmetrically to specimen in order to show any influence of the scan position on the test results.

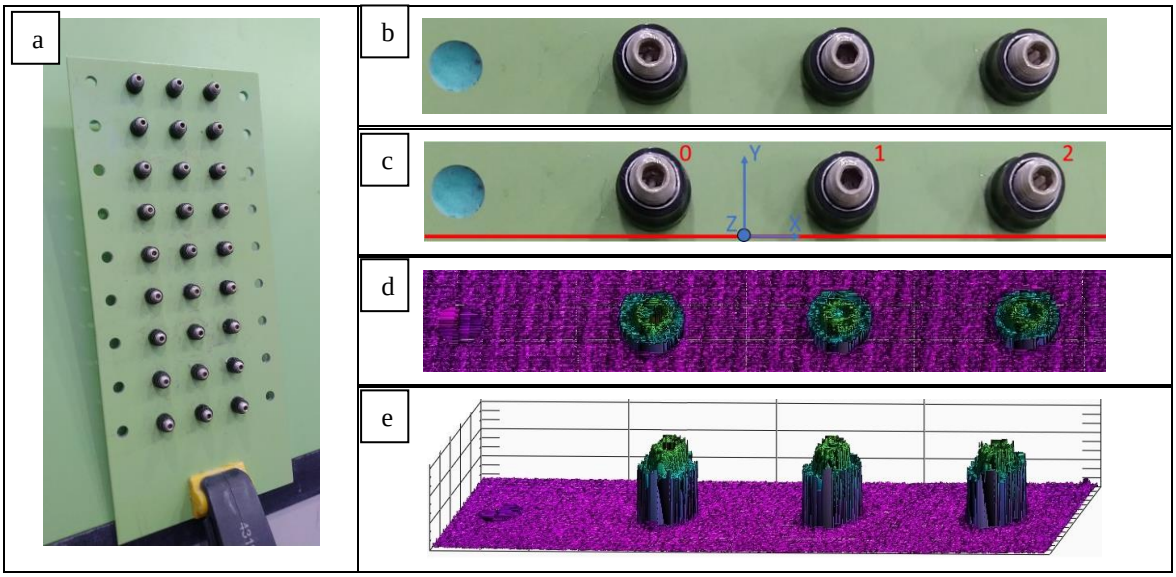

Figure 2. (a) real test board; (b) real scanned specimen; (c) real scanned specimen with scanning reference and fasteners identification; (d) and (e) scan data visualization.

The point cloud obtained by the scanning does not fully reflect all the dimensional characteristics of the specimen, since there are read error from the surface capture by the 2D laser scanner, deviations caused by mechanical vibration of the effector/robot assembly and unseen regions of the surface by the sensor (shading regions). Figure 3a shows the 2D scan with its projection of the laser line on the target surface with its projection angle (Fig. 3b) and sensor receiver return angle (Fig 3c). These angles, depending on the topology of the target surface, cause shading regions not seen by the sensor.

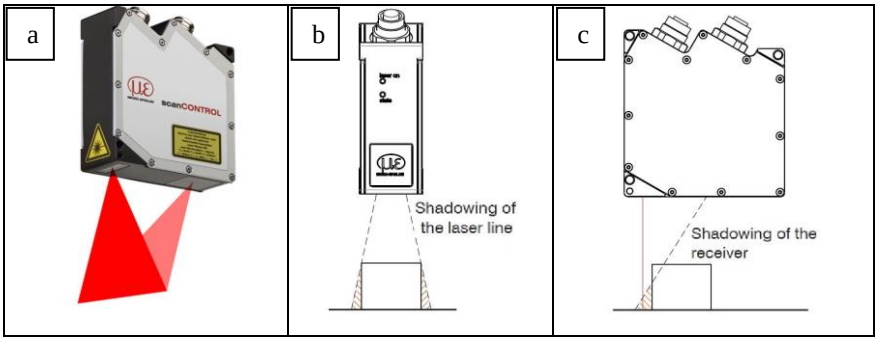

Figure 3. (a) 2D laser scan with its laser line projection signal transmission and reception; (b) Shadowing of the laser line caused by transmission angle; (c) Shadowing of the receiver caused by reception angle (MICRO-EPSILON, 2008)

In this work we opted to carry out the top view scanning of the fasteners with linear movements of the robot in a single pass, therefore without overlapping scanned regions. The scanning methodology is as follows:

1. the 2D laser scanner is positioned perpendicular to the test plate at a known distance in the sensor reading range (Fig. 4a), using the *"Static Methodology"* explained in (Santos et al., 2018);
2. the robotic manipulator performs small linear motion with a set distance (step) in the Y direction;
3. when the robot finishes the movement (step), it sends a message to the desktop computer that stores the 2D scanner's reading. The 2D scanner measures the distances between itself and the surrounding surface in Z direction along a line, around 80.0 at 143.5 mm, dividing this line into up to 640 points in the X direction. Therefore the sensor sends a vector of 640 points (X, Z);
4. when the desktop computer finishes storing the 2D laser scanner information it sends a message to the robot to perform a next move, returning to step 2, or if this is the last step, the operation is terminated, and a file is generated containing the 3D point cloud with collected data.

Due to the known shape of the fastener and its susceptibility to the shadowing errors already reported, in order to reduce this error, a variation of the scanning operation was developed. In scan operation, after performing half of the total scanning steps, the robotic manipulator performs a rotation of his pose in 180 degrees in the Z axis of the scanner sensor at point X = 0. This causes the projected laser line to remain in the same position as before rotation, but the scanner receiver is in a better viewing position of the fastener. This operation was called Scanning Pose Rotation (SPR). After rotation, the scan operation continues until the remaining steps are completed. The scan operation without SPR can be seen in the photos sequence of Fig. 4a, 4b and 4c. The scan made with SPR can be seen in the photos sequence of Fig. 4a, 4b, 4d and 4e.

With the point cloud captured, the analysis software developed in LabView performs a set of filtering and math operations, so that it is possible to transform the data into a three-dimensional matrix where the index of each field represents its dimensional position (XYZ) in space and the value of the field can assume binary values, 0 if it is free, or 1 if it is full. The conversion operations are basically:

- identification of the measuring range for each X-axis data vector (maximum and minimum values);
- identification of a measurement range common to all X-axis data vectors (maximum value of the set of minimum values, and minimum value of the set of maximum values) and calculation of X Span;
- identification of the measurement range of the Y axis data vector (maximum and minimum value) and calculation of Y Span;
- identification of the measurement range of the Z data matrix by identifying the maximum and minimum value between all Z values and calculation of the Z Span;
- creation of a three-dimensional matrix with X, Y and Z lengths calculated by dividing their respective Spans by the chosen resolution of the matrix (in this case 0.1mm);
- identify in the original data (point cloud) the values of Z for each set of X and Y values represented by the index of the three-dimensional matrix (approximation by the nearest value);
- populate the three-dimensional matrix cells with value 1 if Z value represented by its index in the three-dimensional matrix is equal or less than Z value found in original data for a given set X and Y value represented by its index. Otherwise populate with value 0.

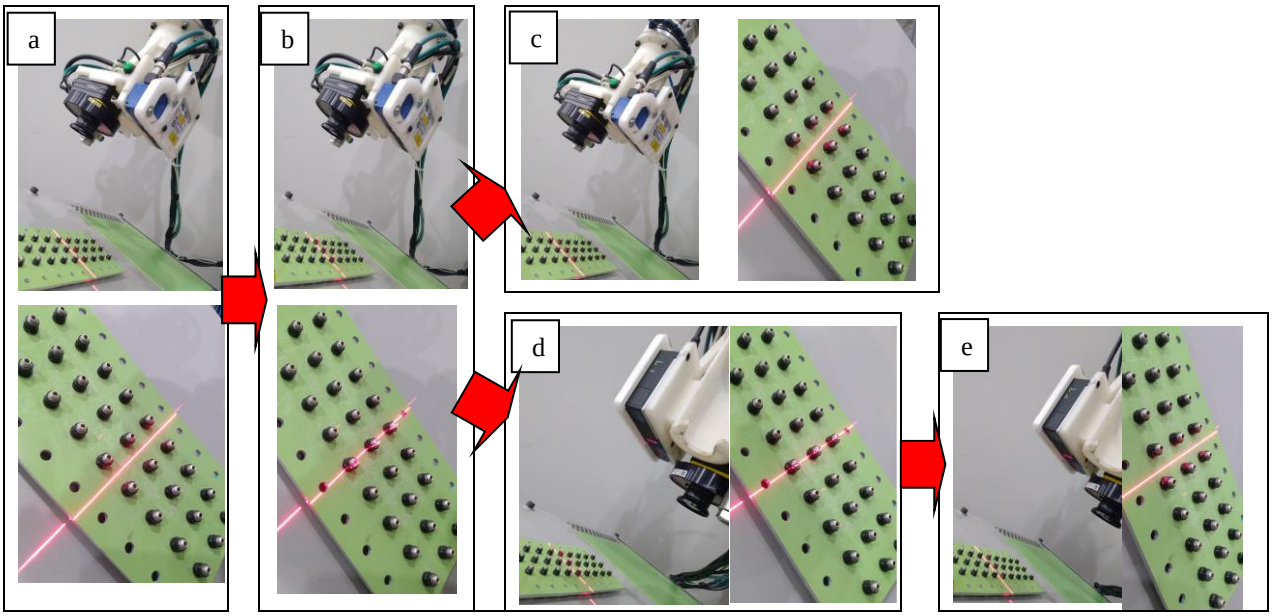

Figure 4. (a), (b) and (c) – sequential photos of scan operation without Scan Pose Rotation (SPR); (a), (b), (d) and (e) - sequential photos of scan operation with Scan Pose Rotation (SPR)

As this three-dimensional binarized matrix it is possible to generate two-dimensional images by capturing matrix data with the same index, X or Y or Z. And then, it is possible to use computational vision techniques, such as blob detection, to separate the fasteners regions that are of our interest, Fig. 5b. After separation of the interest data, the various images extracted in the Z direction are analysed (Fig. 5c) and their edges are extracted (Fig. 5d). As the fasteners are concentric cylindrical structures (Fig. 5a), in order to identify their central position, in each Z-cut image the best fit of a circumference is realized (Fig. 5e). By doing circle best fit in all Z-cut images of the fastener, we now have a set of circles representing the fastener, but which may diverge from their central position as a result of noises and reading errors picked up during the scanning, this error is show in Fig. 5f. Doing its edge extraction (Fig. 5g) generating circles with approximation errors (Fig. 5h).

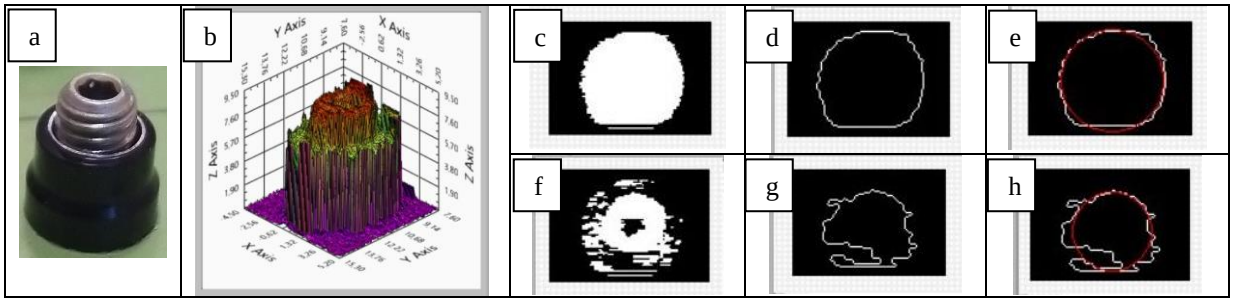

Figure 5. (a) real fastener (b) scan data visualization of fastener; (c) slice Z in 4.0mm of the fastener scanned; (d) extracted border of the slice fastener scanned; (e) circle best fit in slice fastener scanned; (f) slice Z in 6.5mm with error; (g) extracted border of the slice scanned with error and noise; (h) circle best fit in slice with error and noise.

The LabView function used to best fit of a circumference in Z-cut image was the “IMAQ Fit Circle 2 VI”. This function finds the circle that best represents a set of points and returns the radius, perimeter, and area of the circle. This function requires a minimum of three points. The resulting circle may take into account only a subset of the points you provide due to outlier analysis perform. The residual analysis is also made by function that returns the least square error calculate of the fitted circle over every given radial point used.

As the center of the fasteners is unique and we have several circles representing it, some computation methods have been tested to extract this value, they are:

- Best Fit Center Point (BFA): in this method all border points are extracted from all cut-Z images and merged into a new image. From this image is realized a new circle best fit generating a unique circle in which its center and considered the center of the fastener.
- Best Fit Center Point with Selection (BFS): this method is the same that previous one, but only borders of selected circles image are used.

- Average Center Point (AVA): average of the center values of all circles finding;
- Average Center Point with Selection (AVS): average of the center values of circles selected according to low error by diameter criteria.

The selection criteria used in the BFS and AVS methods were:

- best fit circumference that present least square error less than 40mm, and;
- best fit circumference that present ratio between points used (not discarded by outlier analysis) and total points greater than 0.6 (60%).

The cut-off values of the two criteria were chosen empirically. The first criterion allows us to evaluate the dimensional error between the set of points and the best fit circumference. The second criterion allows us to evaluate how closely the set of points are organized in circular form. If the point organization is a perfect circular shape, the IMAQ Fit Circle 2 function will not exclude any points and the second criterion will have a maximum value of 1.0 (100%). If the organization of points is very different from a circle, several points will be classified as outliers and the second criterion will have low value (less than 1.0).

3. THE EXPERIMENT

In order to prove if it is possible to identify the distance between centers of cylindrical fasteners installed in a flat test board with the apparatus developed it was adopted a Design of Experiment (DoE) methodology. The goal is to evaluate what would be the influence of each factor and what would be the best setting that minimizes measurement error.

The experiment develop is a three-factor factorial design, in which the factor and levels are list in Table 1.

Table 1. Experiment Factor and Levels

Factor and Levels of the Experiment				
Factor	**Level 1**	**Level 2**	**Level 3**	**Level 4**
Computational Method (A)	BFA	BFS	AVA	AVS
Fasteners Position (B)	0to1	1to2	2to0	-
Scan Method (C)	0 (w/o SPR)	1 (w/ SPR)	-	-

The selected levels are the variations that the factors may have, which have been tested to verify their influence. The four computational methods developed, the position of the fasteners relative to the scan reference used to measure the distance between centers, and the scanning method with (w/) and without (w/o) pose rotation are tested.

Tests were performed using the methodology already commented and its results were compared with the measurement of the test board in a Coordinate-Measuring Machine (CMM) model Crysta-Apex C 7106 manufactured by Mitutoyo.

The statistical model of the test is presented in Equation 1:

$$y_{ijkl} = \mu + A_i + B_j + C_k + (AB)_{ij} + (AC)_{ik} + (BC)_{jk} + (ABC)_{ijk} + E_{ijkl} \quad (1)$$

Where:

i: i-th factor level {i = 1, 2, 3, 4} - (Computational Method);
j: j-th factor level {j = 1, 2, 3} - (Fasteners Position);
k: k-th factor level {k = 1,2} - (Scan Method);
l: l-th experimental replicates {l = 1,2, …, 9};
y_{ijkl}: distance error between CMM and experimental measurement;
μ: overall mean of y;
A_i: effect of the i-th factor level (Computational Method);
B_j: effect of the j-th factor level (Fasteners Position);
C_k: effect of the k-th factor level (Scan Method);
$(AB)_{ij}$: effect of the interaction of the i-th factor level (Computational Method), and the j-th factor level (Fasteners Position);
$(AC)_{ik}$: effect of the interaction of the i-th factor level (Computational Method), and the k-th factor level (Scan Method);
$(BC)_{jk}$: effect of the interaction of the j-th factor level (Fasteners Position), and the k-th factor level (Scan Method);
$(ABC)_{ijk}$: effect of the interaction of the i-th factor level (Computational Method), the j-th factor level (Fasteners Position), and the k-th factor level (Scan Method);
E_{ijkl}: random error.

For the generation of the required experimental data, the test plate (Fig. 2a) was scanned row by row individually, with the laser scanner positioning being done as shown in (Fig. 2c) using the two scanning methods with Y-direction movements with 0.1mm pitch totaling 200 steps (20mm scanning). Eighteen point cloud files were generated and treated by the analysis software. The value of 0.1mm was used as the resolution of the converted binarized three-dimensional matrix, since the resolution of the readings obtained from the 2D sensor scanner in X-direction varied around this value. Upon completion of the developed software analysis routine, it is returned the results of the central position of each fastener calculated by the four computational methods developed. With the central position of each fastener, the distance between centers of each pair of fasteners is calculated. With the CMM measurement of each fastener position, it is possible to calculate the error between the CMM measurement and the experimentally generated one. The observed variable in ANOVA test is the distance error between CMM and experimental measurement.

4. RESULT AND DISCUSSION

The results obtained from the experiment are summarized in Table 2.

As the nine lines of the test board were scanned, this represents nine replicates of factors level set were made to evaluate the accuracy of each method. The results correspond to the distance error between CMM measurement and those who calculated by mentioned computational methods, with and without scan pose rotation, and with fasteners position classified.

Table 2. Experimental results for find distance between centers fasteners

Row	Distance Between Centers		Distance Error Between Centers [mm] (CMM - CM.SPR)							
			Computational Method (CM)							
	Position Fasteners	CMM [mm]	BFA		BFS		AVA		AVS	
			w/ SPR	w/o SPR	w/ SPR	w/o SPR	w/ SPR	w/o SPR	w/ SPR	w/o SPR
L1	0 to 1 =>	19,981	0,237	0,179	0,274	0,181	0,252	0,237	0,264	0,236
	1 to 2 =>	19,928	0,079	-0,026	0,069	-0,041	0,048	0,041	0,058	0,059
	2 to 0 =>	39,909	0,316	0,153	0,342	0,140	0,300	0,277	0,321	0,294
L2	0 to 1 =>	19,764	0,302	0,213	0,321	0,250	0,334	0,257	0,350	0,306
	1 to 2 =>	19,885	-0,039	-0,117	-0,017	-0,113	0,011	-0,111	0,248	-0,094
	2 to 0 =>	39,646	0,264	0,097	0,305	0,137	0,349	0,149	0,599	0,213
L3	0 to 1 =>	19,813	0,235	0,146	0,201	0,172	0,321	0,157	0,307	0,174
	1 to 2 =>	20,105	0,067	0,029	0,092	-0,026	0,050	0,105	0,095	0,106
	2 to 0 =>	39,918	0,303	0,175	0,293	0,146	0,371	0,263	0,403	0,281
L4	0 to 1 =>	19,849	0,160	0,154	0,181	0,183	0,256	0,258	0,243	0,269
	1 to 2 =>	20,072	0,146	-0,028	0,259	0,027	0,120	0,035	0,400	0,059
	2 to 0 =>	39,920	0,305	0,126	0,440	0,210	0,376	0,293	0,646	0,328
L5	0 to 1 =>	19,892	0,153	0,070	0,165	0,093	0,156	0,188	0,186	0,210
	1 to 2 =>	19,998	0,096	-0,036	0,063	-0,033	0,115	-0,126	0,120	-0,060
	2 to 0 =>	39,890	0,250	0,034	0,228	0,060	0,272	0,063	0,307	0,150
L6	0 to 1 =>	19,810	0,154	0,098	0,151	0,101	0,258	0,227	0,232	0,161
	1 to 2 =>	20,128	0,145	0,140	0,306	0,051	0,051	0,114	0,352	0,111
	2 to 0 =>	39,938	0,299	0,239	0,458	0,152	0,309	0,341	0,585	0,272
L7	0 to 1 =>	20,072	0,313	0,195	0,319	0,182	0,398	0,230	0,407	0,246
	1 to 2 =>	19,772	-0,019	-0,052	0,033	-0,089	0,055	-0,031	0,095	0,008
	2 to 0 =>	39,842	0,292	0,141	0,352	0,093	0,454	0,198	0,504	0,255
L8	0 to 1 =>	19,869	0,264	0,149	0,222	0,128	0,198	0,163	0,238	0,180
	1 to 2 =>	19,941	0,116	-0,002	0,193	0,008	0,104	-0,026	0,267	-0,026
	2 to 0 =>	39,811	0,379	0,146	0,414	0,136	0,301	0,137	0,504	0,154
L9	0 to 1 =>	19,861	0,091	0,063	0,120	0,087	0,083	0,127	0,084	0,123
	1 to 2 =>	20,139	0,284	0,139	0,286	0,169	0,228	0,094	0,238	0,102
	2 to 0 =>	39,997	0,374	0,202	0,405	0,256	0,310	0,219	0,320	0,223

The following acronyms are used in Table 2:

w/ SPR: with Scan Pose Rotation.

w/o SPR: without Scan Pose Rotation

The statistical software R is used to analyse the data obtained from the experiment. A first analysis is made by drawing a box plot by combining all levels of the experiment factors (Fig. 6). It provides an estimation of the quality of set of factors.

By analyzing the boxplot graph, it is possible to observe the median and dispersation of the errors according to the desired analysis parameters. We can see that the smallest median of the errors (close to zero) were reached with the following parameters: - AVA.1to2.0; AVS.1to2.0; BFA.1to2.0; and BFS.1to2.0. The sample BFA.1to2.0 have the lowest variability among the samples with the best results. The worst result (median near 0.5) was achieved by AVS.2to0.1, that have also the worst variability.

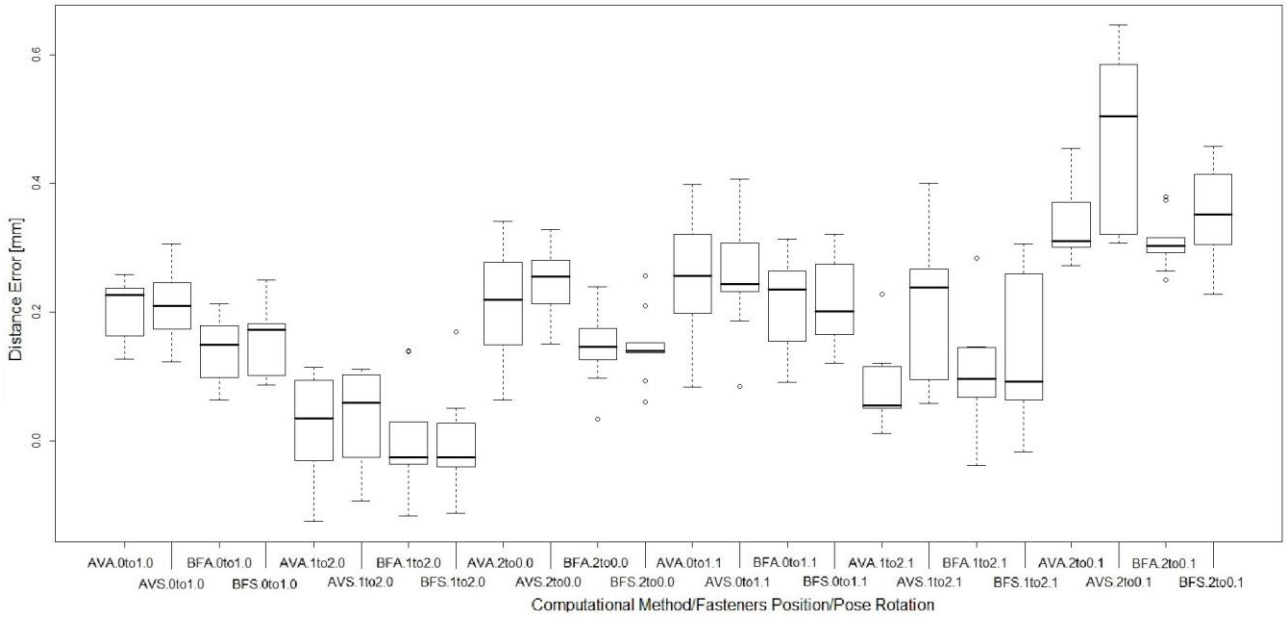

Figure 6. Box Plot of Distance Error by factors Computational Method, Fasteners Position and Scan Pose Rotation

The analysis of variance, ANOVA (Montgomery, 2013), is applied to confirm the influence of the factors on the achieved accuracy. Results are presented in Fig. 7.

	Df	Sum Sq	Mean Sq	F value	Pr(>F)	
a	3	0.2107	0.0702	10.688	1.57e-06	***
b	2	1.5733	0.7867	119.739	< 2e-16	***
c	1	0.7810	0.7810	118.873	< 2e-16	***
a:b	6	0.0515	0.0086	1.306	0.256	
a:c	3	0.0394	0.0131	2.001	0.115	
b:c	2	0.1385	0.0692	10.538	4.55e-05	***
a:b:c	6	0.0234	0.0039	0.593	0.736	
Residuals	192	1.2614	0.0066			

Signif. codes: 0 '***' 0.001 '**' 0.01 '*' 0.05 '.' 0.1 ' ' 1

Figure 7. ANOVA results

It is analysed the three factors and its interactions. The Df (Degrees of Freedom) is defined by n – 1, where n is the total number of levels in the factor, as described previously. The P-Value (Pr) represents the minimal confidence level that is necessary to reject the null hypothesis that is all experimental mean of levels in a factor statistically have the same mean value. ANOVA results show that factors A, B, C and the interaction between factors B and C (BC) influence the experimental error, because its P-Value is much smaller than 1% (0.01), which is the confidence level used in this work. It clearly shows that the three factors are a relevant to influences the experimental error.

To analyze the influence of the levels on each factor found by ANOVA, in Fig. 8 boxplot graphs were placed for each of them. Also was made a Tukey test for analysing the difference between pairs of levels. The results are presented in Fig. 8e. In this test, comparisons between levels with P value less than 1% (0.01) will be considered statistically different.

Considering the significance level of 1% (0.01), the Turkey test (Fig. 8e) and box Plot graphs (Fig. 8a, 8b, 8c and 8d) shows us that:

- the Computational Methods AVA, BFA and BFA are statistically equal and the AVS method differs from the others and it presents worse behaviour (greater variability and median) that can be observed in the box plot Fig. 8a. In Figure 8e the lines marked in blue refer to the AVS level comparisons;
- the Scan Fasteners Position levels differ statistically from each other (Fig. 8e), and the best scan positions in order are 1to2, 0to1 and 2to0 (Fig. 8b);
- the scanning without pose rotate (Fig 8c level equal zero) are better that with pose rotate (Fig. 8c level equal one). It presents less median and variability, and it is statistically different from the other (Fig. 8e lines marked in green);
- in Figure 8d the level (1to2.0), which is the combination of the fasteners position (1to2) and scanning without pose rotation (0) factors, potentiates their effects in decreasing the experimental measurement error, which level is statistically different from the others, as shown in Fig. 8e lines marked in red.

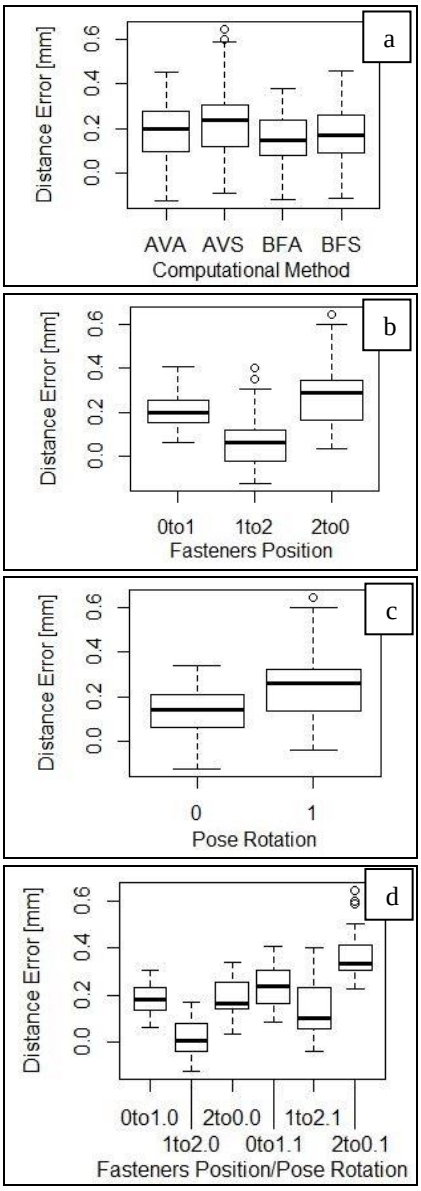

e

```
  Tukey multiple comparisons of means
    99% family-wise confidence level

Fit: aov(formula = y ~ a * b * c)

$a
              diff          lwr         upr     p adj
AVS-AVA  0.05100000  0.001791276  0.10020872 0.0069416
BFA-AVA -0.03270370 -0.081912428  0.01650502 0.1579062
BFS-AVA -0.01525926 -0.064467984  0.03394947 0.7620185
BFA-AVS -0.08370370 -0.132912428 -0.03449498 0.0000014
BFS-AVS -0.06625926 -0.115467984 -0.01705053 0.0001960
BFS-BFA  0.01744444 -0.031764280  0.06665317 0.6786993

$b
                diff         lwr         upr p adj
1to2-0to1 -0.13401389 -0.17384489 -0.09418288 0e+00
2to0-0to1  0.07194444  0.03211344  0.11177545 8e-07
2to0-1to2  0.20595833  0.16612733  0.24578934 0e+00

$c
        diff       lwr       upr p adj
1-0 0.1202593 0.0915626 0.1489559     0

$`b:c`
                        diff          lwr          upr     p adj
1to2:0-0to1:0 -0.16758333 -0.232812531 -0.10235414 0.0000000
2to0:0-0to1:0  0.01000000 -0.055229197  0.07522920 0.9951935
0to1:1-0to1:0  0.05658333 -0.008645864  0.12181253 0.0397320
1to2:1-0to1:0 -0.04386111 -0.109090309  0.02136809 0.2008241
2to0:1-0to1:0  0.19047222  0.125243025  0.25570142 0.0000000
2to0:0-1to2:0  0.17758333  0.112354136  0.24281253 0.0000000
0to1:1-1to2:0  0.22416667  0.158937469  0.28939586 0.0000000
1to2:1-1to2:0  0.12372222  0.058493025  0.18895142 0.0000000
2to0:1-1to2:0  0.35805556  0.292826358  0.42328475 0.0000000
0to1:1-2to0:0  0.04658333 -0.018645864  0.11181253 0.1484389
1to2:1-2to0:0 -0.05386111 -0.119090309  0.01136809 0.0586701
2to0:1-2to0:0  0.18047222  0.115243025  0.24570142 0.0000000
1to2:1-0to1:1 -0.10044444 -0.165673642 -0.03521525 0.0000057
2to0:1-0to1:1  0.13388889  0.068659691  0.19911809 0.0000000
2to0:1-1to2:1  0.23433333  0.169104136  0.29956253 0.0000000
```

Figure 8. (a) Box Plot of the Distance Error by Computational Method; (b) Box Plot of the Distance Error by Fasteners Position; (c) Box Plot of the Distance Error by Scanning Method; (d) Box Plot of the Distance Error by Interaction between Fasteners Position and Scanning Method; (e) Tukey Test results

In order to detect systematic errors introduced in the experiment, we checked the residues. The normality graph of the residues is presented in Fig. 9 and confirms the absence of systematic errors. The residual is considered graphically normal when the points scattered on the plot resembles a straight line and do not show any trend.

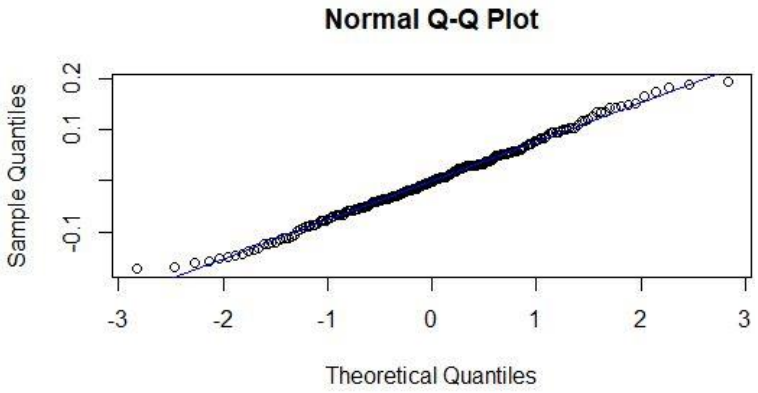

Figure 9. Normality residue Test

Finally, the results of Shapiro-Wilk test for the residual normality confirmed the residual normality, Fig. 10. The P-Value of 54.41% shows us that the null hypothesis is not rejected, and the residuals correspond in fact to random error.

```
        Shapiro-Wilk normality test

data:  res
W = 0.99403, p-value = 0.5441
```

Figure 10. Normality residue Test

5. CONCLUSIONS

This paper presents a non-contact inspection method based on 3D scanning using an industrial robotic manipulator integrated with a 2D laser scanner sensor for measuring the distance between centers of fasteners installed on a flat plate. Computational algorithms were used to extract the desired information from the data generated during the scanning phase. To evaluate the methodology created, a three-factor factorial experiment was designed to prove the effectiveness of the method and answer the question of what would be the best configuration of techniques to minimize the measurement error.

The results obtained in the designed experiment shows that the inspection method is effective in measuring the distance between centers of cylindrical fasteners on a flat plate with median error equal to -0.04mm and variability of approximately 0.18mm for the set of factors that obtained the best results (1to2.BFA.0). This result is considered good as the measurement resolution of the 2D laser scanning sensor in X-direction is approximately 0.1mm.

In the experiment, it was found that the scanning position influences the experimental error. As in a scanning operation it is possible to scan up to four fasteners of the dimension used in this work, it is possible to evaluate if the error for each position is permissible, with the best results by position:

- Position 0to1: median equal to 0.18mm and variability equal to 0.15mm (0to1.BFA.0);
- Position 1to2: median equal to -0.04mm and variability equal to 0.18mm (1to2.BFA.0);
- Position 2to1: median equal to 0.18mm and variability equal to 0.15mm (2to1.BFA.0);

Another possible conclusion is that the scan with pose rotation presented worse results than the one without rotation. A possible cause would be the additional movement during the pose shifting of the robotic manipulator that have repeatability equals +/- 0.1mm (Kuka, 2015) and that although the fastener dimensional profile is susceptible to receiver shading errors, they are not significant.

As for the computational algorithms for extracting the distance between centers, the AVA, BFA and BFS algorithms presented similar medians and variabilities, being proved by Tukey test that they are statistically similar, and they were considered of good yield. Already the AVS algorithm presented higher variability, being considered the worst yield among the other.

As future work, we plan to investigate other dimensional parameters that can be stratified using the method develop.

6. ACKNOWLEDGEMENTS

The authors thank the financial support from Brazilian funding agencies CAPES, CNPq and FINEP.

7. REFERENCES

Cao, H., Sun, H., Jia, Q., Ye, P., & Shi, C. (2009). Laser-scanner grid map building based on Dempster-Shafer evidence theory. *2009 IEEE International Conference on Mechatronics and Automation, ICMA 2009*, *2*(C), 4930–4935. https://doi.org/10.1109/ICMA.2009.5246030

Chu, H., Gong, K., Shao, Y., Chang, Z., & Ni, J. (2018). 3D Perception and Reconstruction System Based on a 2D Laser Scanner. In *Chinese Automation Congress (CAC)* (Vol. 2018, pp. 1520–1524). Xi'an, China: IEEE. https://doi.org/10.1109/CAC.2018.8623391

Di Angelo, L., Di Stefano, P., & Morabito, A. E. (2019). Fillets, rounds, grooves and sharp edges segmentation from 3D scanned surfaces. *Computer-Aided Design*, *110*, 78–91. https://doi.org/10.1016/j.cad.2019.01.003

Haleem, A., & Javaid, M. (2018). 3D scanning applications in medical field: A literature-based review. *Clinical Epidemiology and Global Health*, (May), 0–1. https://doi.org/10.1016/j.cegh.2018.05.006

Huhle, B., Schairer, T., Schilling, A., & Straßer, W. (2011). 6DoF registration of 2D laser scans. *Proceedings - 2011 International Conference on 3D Imaging, Modeling, Processing, Visualization and Transmission, 3DIMPVT 2011*, 148–155. https://doi.org/10.1109/3DIMPVT.2011.26

Lavrinov, D. S., & Khorkin, A. I. (2016). Problems of internal calibration of precision laser triangulation 2D scanners. *2016 2nd International Conference on Industrial Engineering, Applications and Manufacturing, ICIEAM 2016 - Proceedings*, 1–4. https://doi.org/10.1109/ICIEAM.2016.7910962

Lavrinov, D. S., & Khorkin, A. I. (2017). Laser Triangulation 2D Scanner Signal Processing for Premium Thread Pitch Measurement. In *2017 International Conference on Industrial Engineering, Application and Manufacturing (ICIEAM)*. St. Petersburg, Russia. https://doi.org/10.1109/ICIEAM.2017.8076110

Kuka Robotics Corporation (2015). LBR IIWA 7 R820 LBR Specifications. http://www.kuka-robotics.com/res/sps/e6c77545-9030-49b1-93f5-4d17c92173aa_Spez_LBR_iiwa_en.pdf. Accessed in July 27, 2019

MICRO-EPSILON. (2008) Instruction Manual scanCONTROL 26xx. Available in: <https://www.micro-epsilon.com/download/manuals/man--scanCONTROL-26xx--en.pdf>. Accessed in June 11, 2019

Montgomery, D.C. (2013). Design and Analysis of Experiments. 8 ed. 111 River Street, Hoboken, NJ: John Wiley & Sons, Inc, 2013.

Phan, N. D. M., Quinsat, Y., Lavernhe, S., & Lartigue, C. (2018). Path Planning of a Laser-scanner with the Control of Overlap for 3d Part Inspection. *Procedia CIRP*, *67*, 392–397. https://doi.org/10.1016/j.procir.2017.12.231

Rao, M. R., Radhakrishna, D., & Usha, S. (2018). Development of a Robot-mounted 3D Scanner and Multi-view Registration Techniques for Industrial Applications. *Procedia Computer Science*, *133*, 256–267. https://doi.org/10.1016/j.procs.2018.07.032

Santos, K. R. da S., Tricarico, R. T., Suterio, R., Ferreira, L. F. L. R., de Carvalho, G. M., & Villani, E. (2018). Evaluation of perpendicularity methods for a robotic end effector from aircraft industry. In *2018 13th IEEE International Conference on Industry Applications* (pp. 1373–1380). São Paulo, Brazil. https://doi.org/10.1109/induscon.2018.8627218

Vina, C., & Morin, P. (2017). Model-based pose estimation on-board MAVs equipped with 2D laser scanners for the automatic inspection of electric towers. *11th International Workshop on Robot Motion and Control, RoMoCo 2017 - Workshop Proceedings*, 78–84. https://doi.org/10.1109/RoMoCo.2017.8003895

Wang, X., Li, H., & Liu, B. (2017). Object tracking and state estimation in outdoor scenes based on 3D laser scanner. *2016 IEEE International Conference on Signal and Image Processing, ICSIP 2016*, 607–611. https://doi.org/10.1109/SIPROCESS.2016.7888334

Yamada, T., Ito, T., & Ohya, A. (2014). Detection of road surface damage using mobile robot equipped with 2D laser scanner. *Proceedings of the 2013 IEEE/SICE International Symposium on System Integration*, 250–256. https://doi.org/10.1109/sii.2013.6776679

Zhang, H., Rong, X., Li, B., & Li, Y. (2017). Leader Recognition Based on 2D Laser Scanner and Pan-Tilt for Quadruped Robots. In *Chinese Automation Congress (CAC)* (pp. 5052–5056). Jinan, China. https://doi.org/10.1109/CAC.2017.8243676

8. RESPONSIBILITY NOTICE

The authors are the only responsible for the printed material included in this paper.